Materials Research, Vol. 7, No. 1, 27-33, 2004.

Composite Coatings of Titanium-Aluminum Nitride for Steel against Corrosion Induced by Solid NaCl Deposit and Water Vapor at 600 °C

M.S. Li, F.H. Wang, Y.H. Shu, W.T. Wu*

State Key Laboratory for Corrosion and Protection
Institute of Metal Research, The Chinese Academy of Sciences
Wencui Road 62, 110016 Shenyang, China

Received: September 2, 2002; Revised: September 4, 2002

Composite coatings (Ti,Al)N with different Al content were deposited on a wrought martensite steel 1Cr11Ni2W2MoV by reactive multi-arc ion plating. With the addition of Al to the coatings, the crystallographic structure of them changed from B1 NaCl to B4 ZnS, the relevant hardness and adhesive strength firstly increased then decreased and their oxidation-resistance was also dramatically improved. It was indicated that the introduction of Al was beneficial to (Ti,Al)N coatings against corrosion induced by NaCl(s) in wet oxygen at 600 °C as well as wet corrosion in NaCl solution at ambient temperature.

Keywords: *coatings (Ti,Al)N, steel, synergistic effect, NaCl, water vapor, corrosion*

1. Introduction

It was observed that serious corrosion occurred on the compressor blades of the higher stages in a gas turbine engine after service for a long period of time in marine environment[1,2]. The compressor blades were made of a martensite steel 1Cr11Ni2W2MoV and operated at temperature around 450~600 °C. This type of corrosion may be induced by sea water vapor or by the synergistic effect of solid salt deposits and water vapor. NaCl is one of the major components of salt deposits which, accumulated on the material surface in the field. In a primary study it is revealed that solid NaCl deposits and water vapor may have a strong synergistic effect on the corrosion of Cr containing steels in air at intermediate temperatures 500-600 °C, as well as that of pure Fe and Cr, and even CrN[1-4]. However, TiN showed corrosion resistance to this severe corrosive environment to some extent[1]. But TiN can be oxidized rapidly in air at temperature above 550 °C [5,6]. In order to search for better coatings for Cr containing steel, a further study on preparation by reactive multi-arc ion plating and characterization of coatings (Ti,Al)N was performed. The main results of characteristics of the coatings are briefly summarized in this article.

*e-mail: wwt@imr.ac.cn
Presented at the International Symposium on High Temperature Corrosion in Energy Related Systems, Angra dos Reis - RJ, September 2002.

2. Experimental Procedure

The substrate material is the wrought martensite steel 1Cr11Ni2W2MoV (nominal compositions, wt%: C 0.1-0.16, Cr 10.5-12, Ni 1.4-1.8, W 1.5-2, Mo 0.35-0.5, V 0.18-0.30, Mn 0.6, Si 0.6, S 0.02 and P 0.03). The samples were cut into 15 mm × 10 mm × 2 mm and ground to 1000 grit for test. Just before the experiment, the specimens were degreased in acetone, ethanol and dried in air.

Titanium aluminum nitride coatings with different Al content were deposited on steel specimens by a homemade reactive multi-arc ion plating facility of AIP-800-8 Coating System. Targets of pure Ti and Ti-Al alloys with different Al content were used respectively. Before depositing, the substrates were pre-cleaned by sputtering with Ar ions under –1000 V bias voltage. The deposition parameters were listed as following: Deposition temperature 400~450 °C, Total pressure 1.0 Pa, N_2 partial pressure 0.6 Pa, Arc voltage 20 V, Arc current 60A, D.C pulse bias voltage –450 V and Duty cycle 30%.

The composition of coatings was analyzed by electron probe microanalysis (CAMEBAX-MICTO). The phase constituent of coatings was characterized by X-ray diffraction

(XRD) with CuK_α radiation. The hardness of coatings was measured by an ultra micro-hardness tester (CHX-1), which allows loading down to 10 g. A Scratch Tester equipped with Rockwell C diamond tip was used to evaluate the adhesive strength of coatings.

The onset temperature of oxidation of coatings was measured by thermo-balance in air with a heating rate 2 °C/min from room temperature to 850 °C. For corrosion test, the specimen surface was pre-placed with NaCl around 0.6 mg/cm^2. Then the sample was tested at 600 °C with a thermo-balance equipped with a system of water vapor control to offer the reaction chamber an O_2 flow with 12 vol.% water vapor, and the test procedures were described elsewhere[1,2,7]. Potentiodynamic polarization curves were also measured with a potentiostat M273 for steel without and with coatings in NaCl solution.

3. Results and Discussion

3.1 Crystallographic structure of coatings (Ti,Al)N

A series of coatings (Ti_{1-x},Al_x)N with Al fraction x = 0, 0.09, 0.20,0.26, 0.33, 0.50, 0.64., 0.79 and 0.92 were prepared respectively.

Figure 1 shows the XRD patterns of the coatings (Ti,Al)N with various Al content. It is clear that the crystallographic structure of the coatings (Ti,Al)N is B1 NaCl type phase TiN when Al fraction below x = 0.65, and above which transforms to B4 ZnS type phase AlN and at x = 0.65 it is a mixture of the two phases. The preferential orientation in coatings (Ti,Al)N of B1 phase changes from (111) to (220) with the increase of Al content. For both B1 NaCl phase and wurtzite phase, the peaks of XRD pattern gradually shifted to higher diffraction angle in proportion to the x value, signifying that the lattice parameter decreased with the addition of Al. Ikeda *et al.*[5] attributed the change of the lattice parameter to the substitution of Al atoms with the Ti atoms since coatings (Ti,Al)N can be considered as a solid solution in which Al atoms were substituted for Ti sites in B1 structure while Ti atoms were substituted for Al sites in B4 structure.

3.2 Hardness and adhesive strength of coatings (Ti,Al)N

The micro-hardness and critical scratch load of the coatings were represented as functions of aluminum content as shown in Fig. 2. The hardness of TiN coating with B1 structure is about 2300 H_V. With the addition of Al the microhardness gradually increased up to a maximum value of 3300 H_V at x=0.33. The critical scratch loads slightly increase when x increased from 0 to 0.5, and after which decreased with the increasing aluminum content. It was reported that the hardness of nitrides was influenced by the valence electron concentration (VEC) per unit cell[8]. According to the calculation, the VEC value of $Ti_{0.67}Al_{0.33}N$ is about 8.4. Konig *et al.* have reported that an optimum hardness could be obtained by valence electron concentration range

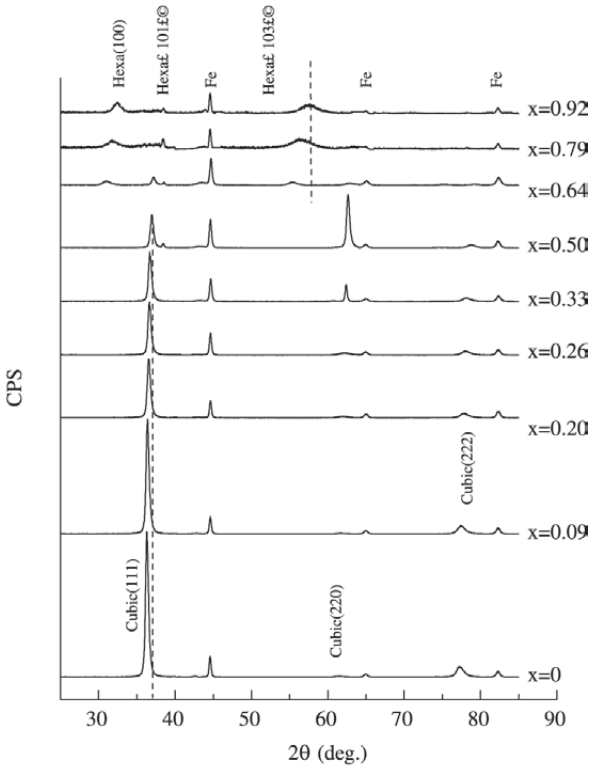

Figure1. XRD pattern of coatings (Ti, Al)N with different Al content.

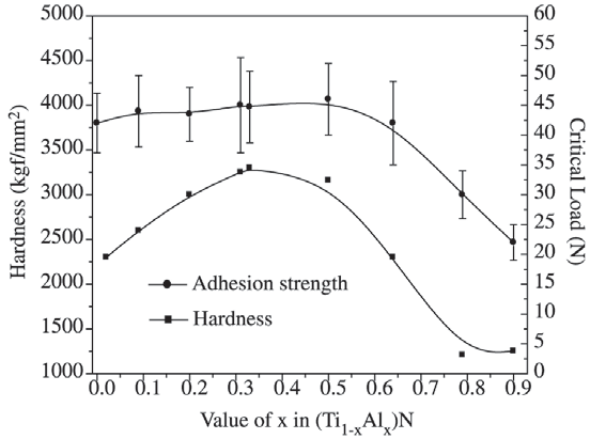

Figure 2. Hardness and adhesion strength of coatings (Ti, Al)N *vs.* Al content.

of 8.4-8.6 for ternary coatings[9]. The hardness of (Ti,Al)N rapidly decreases when x > 0.5, which may be attributed to the phase change.

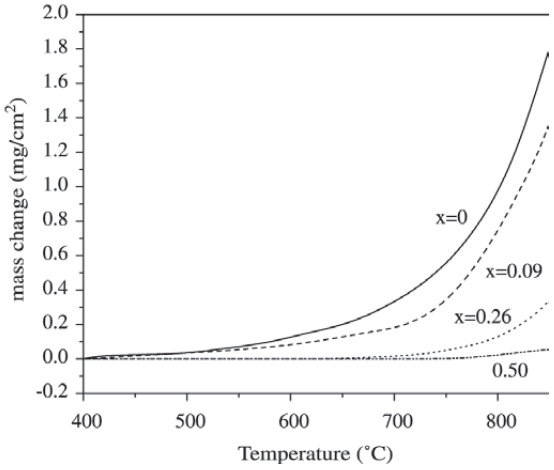

Figure 3. Oxidation curve of coatings $(Ti_{1-x}Al_x)N$ with different Al contents.

3.3 Oxidation-resistance of coatings (Ti,Al)N

Oxidation curves (Fig. 3) indicated that the initiation of oxidation of TiN coating occurred at about 550 °C and which notably increased with the increasing Al content and rose up to above 850 °C when x=0.5. It was manifested from Fig. 4 that the grain size of oxide scale became finer with the increasing Al content. For $Ti_{0.5}Al_{0.5}N$ coating, no extensive change was observed after oxidation. XRD and EDX analysis indicated that an external scale of rutile TiO_2 formed on TiN, but of a mixture of TiO_2 and Al_2O_3 on $Ti_{0.91}Al_{0.09}N$ and $Ti_{0.74}Al_{0.26}N$, then of merely Al_2O_3 on $Ti_{0.5}Al_{0.5}N$. Cross section morphologies of (Ti,Al)N coatings after oxidation were shown in Fig. 5. The whole TiN coating was completely oxidized into TiO_2 and Cr_2O_3 was formed on the interface between substrate and the exhaust coating. With the increase of Al content, the thickness of oxide scale became thinner and denser.

XPS analysis results (Fig. 6) clearly indicated that an Al_2O_3 scale was formed on the surface of $(Ti_{0.5}Al_{0.5})N$. This compact alumina scale seems to prevent further oxidation of the coating. Moreover, it may be suggested from results of theoretical calculation and XPS measurement that the

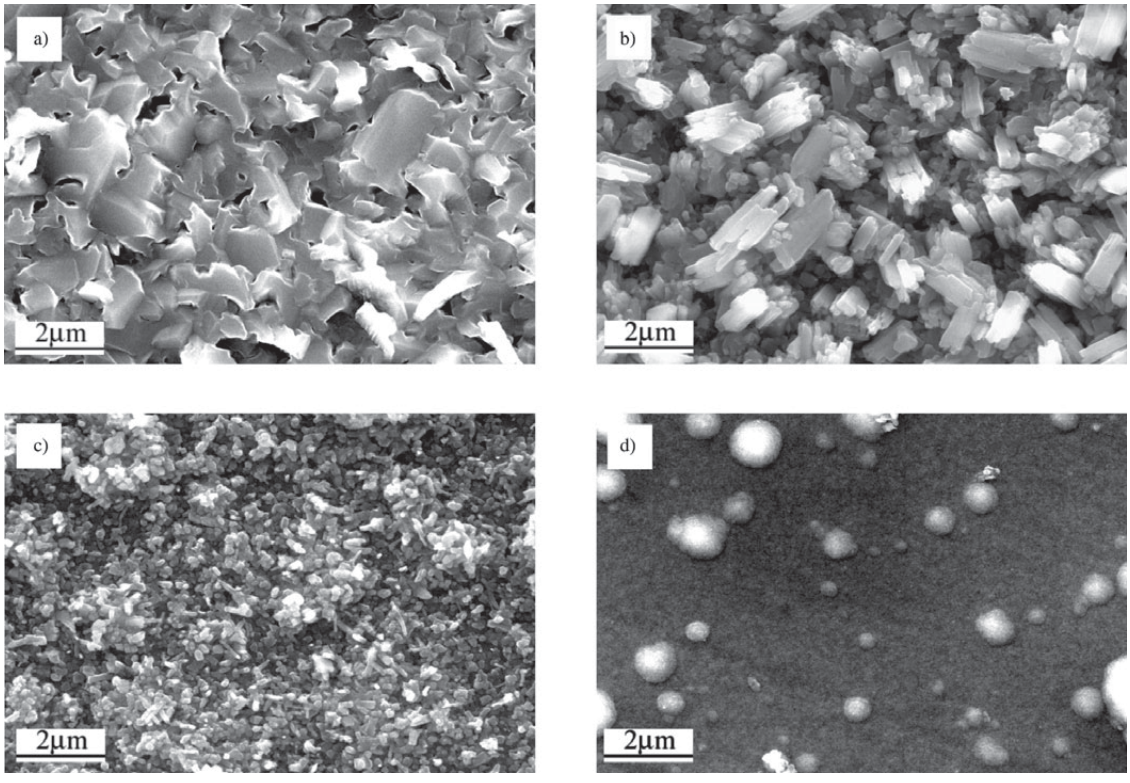

Figure 4. SEM topographies of coatings $(Ti_{1-x}Al_x)N$ after oxidation a) x = 0; b) x = 0.09; c) x = 0.26; d) x=0.50.

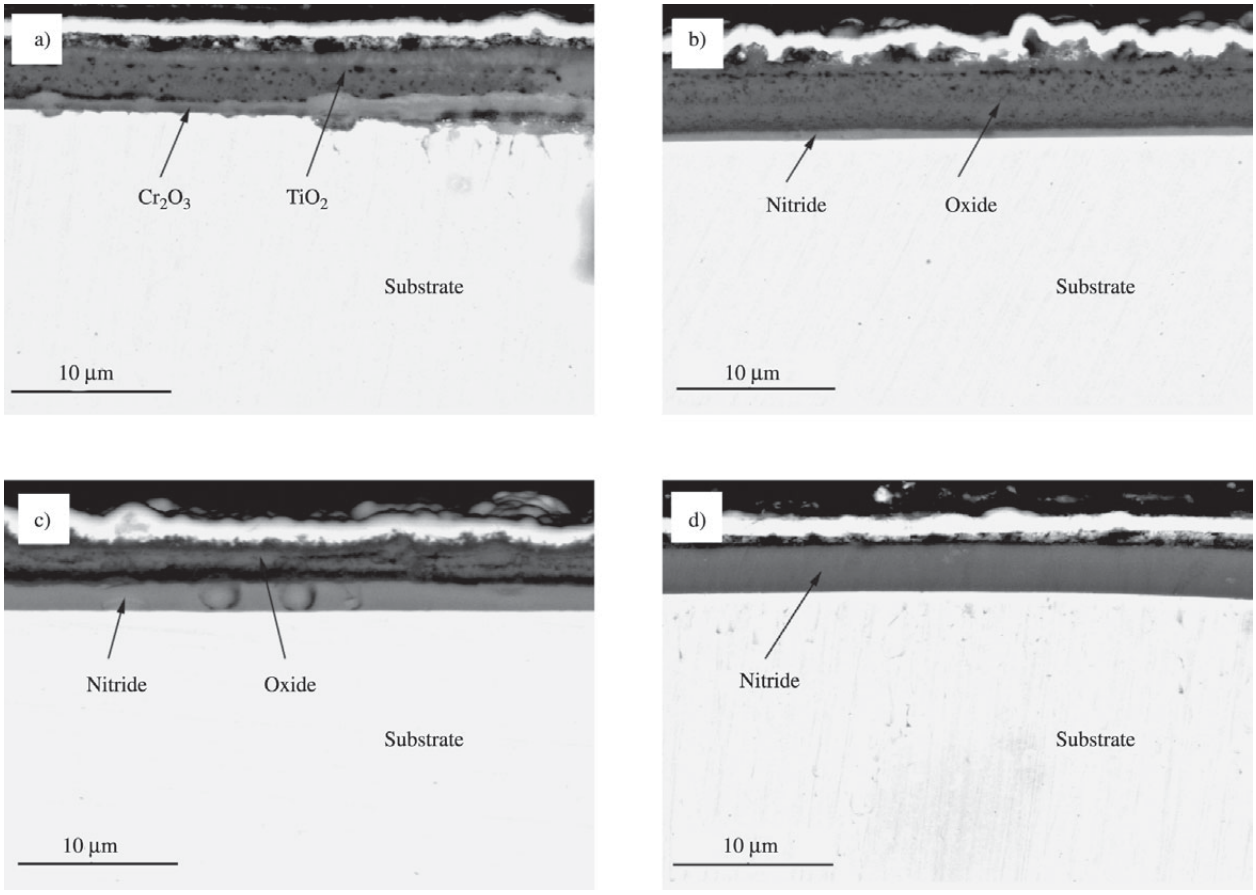

Figure 5. Cross section of coatings $(Ti_{1-x}Al_x)N$ after oxidation a) x = 0; b) x = 0.09; c) x=0.26; d) x=0.50.

reactivity of titanium in the coatings (Ti,Al)N would be suppressed because the valence electron of titanium became more stable in the B1-structure lattice due to the incorporation of Al [10].

3.4 Corrosion of 1Cr11Ni2W2MoV without and with coatings (Ti,Al)N under synergistic effect of water vapor and NaCl deposit

Figure 7 showed the corrosion kinetics of stainless steel 1Cr11Ni2W2MoV with and without coatings under the synergetic effect of NaCl deposit and water vapor. The corrosion of the steel without coating was much severer than that with coatings TiN or (Ti,Al)N. The oxide scale formed on steel 1Cr11Ni2W2MoV was rough and irregular, some parts of which peeled or cracked as shown in Fig. 8a. XRD patterns indicated that the outer part of the scale was mainly Fe_2O_3. Cross sectional morphology and element mapping (see Fig. 8) [1] showed that the oxide scale was thick with layered structure. The outer part of the scale was very porous rich in Fe and followed were successive thinner layers

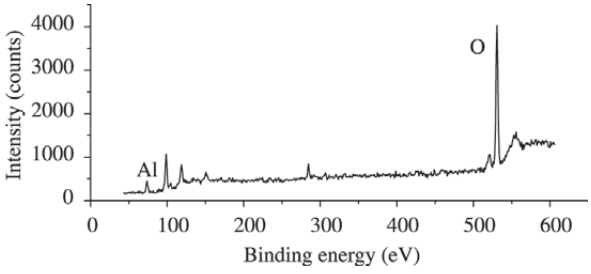

Figure 6. X-ray photoelectron spectra of coating $Ti_{0.5}Al_{0.5}N$ after oxidation.

rich in Cr and Fe alternatively.

A number of nodules with crakes appeared on the TiN surface, which were formed due to the corrosion of the substrate material through pinholes existed in the coating. Oxide scale with finer grains was formed on the coating $Ti_{0.7}Al_{0.3}N$. Since the corrosion was very slight, mass change

could hardly be manifested on the kinetic curve. For the coating $Ti_{0.5}Al_{0.5}N$ there was no obvious mass gain to be detected during the corrosion process and its surface had no significant change after the corrosion.

The NaCl and water vapor are considered to play an important role in the corrosion process. When corrosion in air or water vapor a protective scale Cr_2O_3 formed through the selective oxidation of Cr of the steel[11]. When water vapor and NaCl deposit were simultaneously presented, the protective oxide scale may be destroyed by reactions such as:

$$2NaCl + 1/2Cr_2O_3 + H_2O(g) + 3/4O_2(g) = Na_2CrO_4 + 2HCl(g) \quad (1)$$

The released HCl will react with the Fe and Cr:

$$Fe + 2HCl = FeCl_2(g) + H_2(g) \quad (2)$$

$$Cr + 3HCl = CrCl_3(g) + 3/2H_2(g) \quad (3)$$

Since the melting temperature of the metal chlorides is lower than that of the corresponding oxides, and chlorides possess high vapor pressures at a given temperature. Therefore, $FeCl_2$ or $CrCl_3$ may migrate outwards and react with oxygen and water vapor:

$$2FeCl_2 + 1/2O_2 + 2H_2O = Fe_2O_3 + 4HCl \quad (4)$$

$$2CrCl_3 + 3H_2O = Cr_2O_3 + 6HCl \quad (5)$$

And the released HCl will react with the Fe_2O_3 and Cr_2O_3 cyclically and the corrosion of the steel is accelerated dramatically.

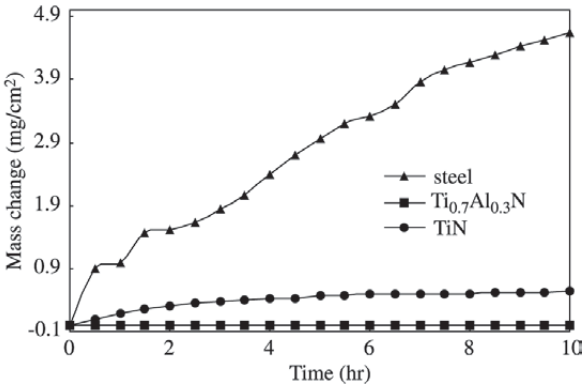

Figure 7. Corrosion kinetics of steel 1Cr11Ni2W2MoV coated with coatings $Ti_{1-x}Al_xN$ under synergistic effect of solid NaCl and water vapor at 600 °C.

At the same time, NaCl and water vapor may react directly with the substrate such as Cr and accelerate the corrosion by following reaction:

$$2NaCl + 4H_2O(g) + 3/2O_2(g) + 2Cr = 1/2Cr_2O_3 + Na_2CrO_4 + 2HCl(g) + 3H_2 \quad (6)$$

On the other hand, according the analysis of Shu *et al.*[1,3], when titanium alloy Ti60 with NaCl deposit is exposed to oxygen plus water vapor at high temperature, corrosion is also accelerated according to the following reactions:

$$2NaCl + Ti + 1/2O_2(g) + H_2O(g) = TiCl_2 + 2NaOH \quad (7)$$

with ΔG^o=-40.98 kJ/mol.

$$TiCl_2 + H_2O(g) = TiO_2 + 2HCl(g) + H_2(g) \quad (8)$$

with ΔG^o =-282.40 kJ/mol.

$$Ti + 2HCl(g) = TiCl_2(g) + H_2(g) \quad (9)$$

with ΔG^o =-102.98 kJ/mol.

If the similar mechanism can be apply to TiN, the corrosion could occur as following reactions:

$$2NaCl + TiN + 1/2O_2(g) + H_2O(g) = TiCl_2(g) + 2NaOH + 1/2N_2(g) \quad (10)$$

with ΔG^o = 239.38 kJ/mol.

$$TiCl_2 + H_2O(g) = TiO_2 + 2HCl(g) + H_2(g) \quad (11)$$

with ΔG^o = -282.4 kJ/mol.

$$TiN + 2HCl(g) = TiCl_2(g) + 2NaOH + H_2(g) + 1/2N_2(g) \quad (12)$$

with ΔG^o = 179.39 kJ/mol.

Herewith it can be seen that the thermodynamic driving force of reaction (10) and (12) is much smaller than that of reaction (7) and (9). Reaction (10) and (12) can hardly progress since the thermo-dynamical balance will be quickly reached. So the simultaneous presence of water vapor and NaCl deposit have no obvious effect on the corrosion of nitrides. Even though there is no distinct difference between the corrosion-resistance induced by the synergistic effect of water vapor and NaCl deposit and the oxidation-resistance in air for nitrides. However the coatings (Ti,Al)N, especially those with high x values showed much better corrosion re-

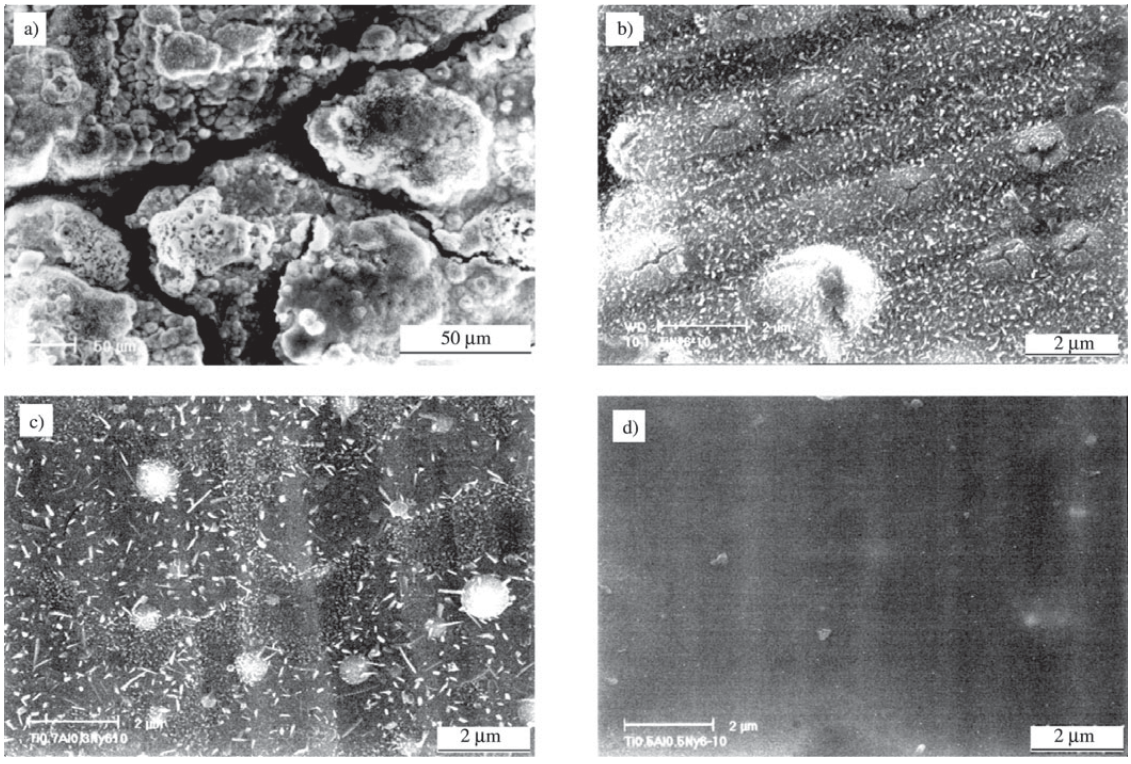

Figure 8. Surface Morphologies of 1Cr11Ni2W2MoV steel with coatings after 10h corrosion at 600 °C under synergistic effect of NaCl and water vapor a) bare steel; b) TiN; c) $Ti_{0.7}Al_{0.3}N$; d) $Ti_{0.5}Al_{0.5}N$.

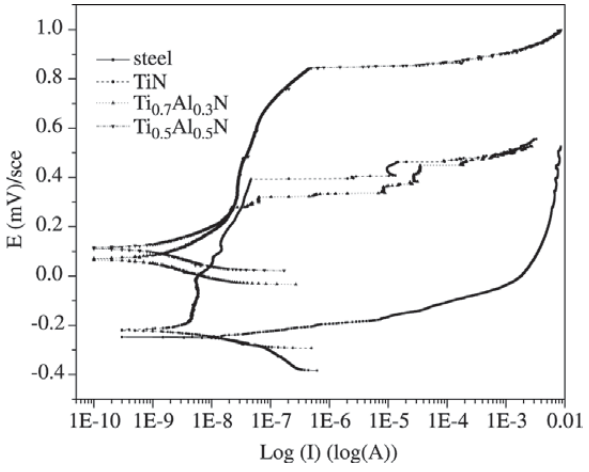

Figure 9. Polarization curves of steel without and with coatings in solution 0.5 M NaCl at ambient temperature.

sistance than TiN. For which the reason may be the preferential oxidation of Al during the very beginning stage of the corrosion, it was which seals pinholes or defects in the coating to prevent the occurrence of any localized nodules-like corrosion as shown in Fig. 8b.

3.6 Wet corrosion performance in NaCl solution at ambient temperature

Potentiodynamic polarization curves in 0.5M NaCl solution (see Fig. 9) indicated that in comparison with the bare steel, the free corrosion potential of nitride coatings shifted to far more positive, especially those with Al additions and they also showed a passivation-like behavior with a wide range of potential. Of course the steel was very susceptible to pitting corrosion in the solution. The fact seemed also important, while in the real service the material may suffer from wet corrosion, especially in the shutdown period of the facility.

4. Conclusions

With addition of Al, the hardness and adhesive strength of coatings (Ti,Al)N may be enhanced, which reach an optimum by certain amount of Al and then decreased.

The oxidation resistance of coatings (Ti,Al)N is enhanced with increasing Al at temperatures up to 800 °C companying with formation of an external scale rich in alumina. Al addition is beneficial also to coatings (Ti,Al)N to protect the

steel 1Cr11Ni2W2MoV against the corrosion induced by solid NaCl in wet oxygen at 600 °C and also the wet corrosion in NaCl solution at ambient temperature.

Therefore, due to the versatility of coatings (Ti,Al)N, it is expected that the chemical composition and phase constituent of the coatings (Ti,Al)N may be tailored to reach an optimal combination of physical and chemical properties to meet the requirements of service.

Acknowledgement

The project supported by NSF China under grants № 59625101 and 59971052.

References

1. Shu, Y.H. *Corrosion behavior of some metals and coatings under the synergetic effect of solid NaCl and water vapor at 500-700 °C*, Doctoral Thesis, The Institute of Corrosion and Protection of Metals. June 1999.
2. Shu, Y.H.; Wang, F.H.; Wu, W.T. *Oxid. Met.*, v. 51, n. 1/2, p. 97-110, 1999.
3. Y. H. Shu, F. H. Wang, and W. T. Wu, *Oxid. Met.*, v. 54, n. 5/6, p. 457-471, 2000.
4. Wu, W.T.; Wang, F.H.; Shu, Y.H. in *High Temp. Corros. Protec 2000*, edited by T. Narita *et. al.*, Science Review, p. 239, 2000.
5. Ikeda, T.; Satoh, H. *Thin Solid Films,* v. 195, p. 99-110, 1991.
6. Cselle, T.; Barimani, A. *Surf. Coat. Technol*. V. 76/77, p. 712-718, 1995.
7. Li, M.S. *Preparation and performance of (Ti,Al)N and (Ti,Al,Y)N coatings deposited by arc ion plating*, Doctoral Thesis, The Institute of Corrosion and Protection of Metals. June 2002.
8. Burg, S.; Blom, H.O.; Larsson, T.; Nender, C. *J. Vac. Sci. Technol.*, A5 (2), p. 202-207, 1987.
9. Konig, U. *Surf. Coatings Technol.*, v. 33, p. 91-103, 1987.
10. Zhou, M.; Makino, Y.; Nose, M.; Nogi, K. *Thin Solid Films,* v. 339, p. 203-208, 1999.
11. Shu, Y.H.; Wang, F.H.; Wu, W.T. *Oxid. Met.*, v. 52, n. 5/6, p. 463-473, 1999.